INRA℮

Annals of Forest Science

Band configurations and seasonality influence the predictions of common boreal tree species using UAS image data

Mikko Kukkonen[1]*, Mari Myllymäki[2], Janne Räty[1], Petri Varvia[3], Matti Maltamo[3], Lauri Korhonen[3] and Petteri Packalen[2]

Abstract

Key message Data acquisition of remote sensing products is an essential component of modern forest inventories. The quality and properties of optical remote sensing data are further emphasised in tree species-specific inventories, where the discrimination of different tree species is based on differences in their spectral properties. Furthermore, phenology affects the spectral properties of both evergreen and deciduous trees through seasons. These confounding factors in both sensor configuration and timing of data acquisition can result in unexpectedly complicated situations if not taken into consideration. This paper examines how the timing of data acquisition and sensor properties influence the prediction of tree species proportions and volumes in a boreal forest area dominated by Norway spruce and Scots pine, with a smaller presence of deciduous trees.

Context The effectiveness of remote sensing for vegetation mapping depends on the properties of the survey area, mapping objectives and sensor configuration.

Aims The objective of this study was to investigate the plot-level relationship between seasonality and different optical band configurations and prediction performance of common boreal tree species. The study was conducted on a 40-ha study area with a systematically sampled circular field plots.

Methods Tree species proportions (0–1) and volumes ($m^3 ha^{-1}$) were predicted with repeated remote sensing data collections in three stages of the growing season: prior (spring), during (summer) and end (autumn). Sensor band configurations included conventional RGB and multispectral (MS). The importance of different wavelengths (red, green, blue, near-infrared and red-edge) and predictive performance of the different band configurations were analysed using zero–one-inflated beta regression and Gaussian process regression.

Results Prediction errors of broadleaves were most affected by band configuration, MS data resulting in lower prediction errors in all seasons. The MS data exhibited slightly lower prediction errors with summer data acquisition compared to other seasons, whereas this period was found to be less suitable for RGB data.

Conclusion The MS data was found to be much less affected by seasonality than the RGB data. Spring was found to be the least optimal season to collect MS and RGB data for tree species-specific predictions.

Keywords Phenology, Photogrammetry, Forest inventory, Drone, Tree species, Multispectral

---

*Correspondence:
Mikko Kukkonen
mikko.kukkonen@luke.fi
Full list of author information is available at the end of the article

BMC

Kukkonen *et al. Annals of Forest Science*   (2024) 81:31

Page 2 of 13

1 Introduction

Information on tree species is beneficial and often necessary for forest inventories and other natural resource monitoring operations. Tree species identification is also required for planning of forest management operations and as inputs for species-specific growth models (Hynynen et al. 2002) or allometric models (Salas-Eljatib et al. 2021). Moreover, tree species are indicators of biodiversity and ecologically valuable habitats (Brockerhoff et al. 2017).

Optical data have been widely utilised for the prediction of tree species (Pu 2021). Optical data are particularly effective for this task due to the interactions between the chemical and physical characteristics of the trees and the amount of reflected radiation that is captured using an optical image sensor (e.g. Hovi et al. 2017). In general, these characteristics are distinctive between tree species, although intraspecific variation exists, for example, between young and old trees (Grabska and Socha 2021), healthy and stressed trees (Masaitis et al. 2013) and dominant and co-dominant trees caused by shadows. Moreover, phenology influences the amount of reflected radiation from both evergreen (Kobayashi et al. 2018) and deciduous trees (Noda et al. 2021). In the context of broadleaved forests, alterations in spectral properties resulting from seasonal changes have been documented within tree species (Blackburn and Milton 1995) and across different tree species (Key et al. 2001).

Phenology can influence the outcome of tree species predictions when data are acquired during life-cycle events (leaf flush and expansion during spring and early summer or leaf senescence and drop in autumn) over vast areas where considerable ecological gradients are present. These events rarely occur for all trees of the same species simultaneously, as there is a large degree of intraspecific variation caused by, for example, genetics, site conditions and competition (Siefert et al. 2015; Cole and Sheldon 2017). These seasonal events can be either detrimental or beneficial for tree species predictions depending on the target tree species, geographical extent, and the time required for data acquisition.

An example of the benefit of phenology in tree species classification was reported by Hardenbol et al. (2021), where the temporal difference in leaf flush between aspen (*Populus tremula* [L.]) and other tree species during late spring was found to be advantageous to discriminate aspen from the other tree species using multispectral (MS) data from an unoccupied aircraft system (UAS). With regard to the classification of deciduous trees, research has shown varying results when data collected during leaf senescence and leaf drop cycles in autumn are compared to other seasons. Hill et al. (2010) found that well timed images captured during autumn provide

better discrimination of broadleaved deciduous tree species than images captured during summer or spring using Airborne Thematic Mapper images (11 bands in the visible, near, short-wave and thermal infrared wavelengths). Persson et al. (2018) reported that late spring Sentinel-2 satellite images were best suited for the discrimination of several broadleaved and conifer tree species. Similarly, Lisein et al. (2015) found that spring and early summer were optimal times to discriminate deciduous tree species using UAS and a consumer-grade red-blue-green (RGB) configuration camera and/or a "modified camera for near infra-red acquisition". They concluded that intraspecific variation in phenology during this period was minor, while interspecific variation, which would be diminished during summer, was still present. In contrast, Weil et al. (2017) presented a method whereby optimal UAS data acquisition dates, with respect to tree species classification, were determined a priori using a time series of near-surface observations. In their eastern Mediterranean study site, they found that late autumn and early winter were the optimal periods to collect data for the classification of the tree species in their study.

The examples provided in the previous paragraph highlight the ambiguity of the interactions between geographical location, tree species, data acquisition time, sensor configuration and successful tree species classification. In general, the best classification performance is obtained at a point in time that minimises the intraspecific variation, while maximising the interspecific differences. However, these periods can be very short, geographically limited, difficult to predict (Cole and Sheldon 2017) and, especially in Nordic countries, restricted by either late spring snow cover or cloud cover. Moreover, late autumn data acquisition should be avoided (Wolter et al. 1995) because during this period the impact of fallen leaves to background reflectance will make distinguishing broadleaved species a more challenging task (Cho et al. 2012).

In addition to influencing reflected radiation, phenology can affect the physical appearance of trees observed via 3D remote sensing techniques, such as photogrammetric point clouds. Huang et al. (2019) found that the height of deciduous trees could be estimated more reliably using leaf-on rather than leaf-off UAS photogrammetric point cloud data. The height estimates of the evergreen tree species investigated in their study were less affected by the seasonality of the remotely sensed data. Bohlin et al. (2017) reported that aircraft-borne photogrammetric point clouds during the leaf-off period were of lesser quality in areas where the proportion of deciduous trees were greatest compared to areas where evergreen tree species predominated. In their study, this led to a large underestimation of deciduous tree volume and the authors recommended against the collection

of leaf-off photogrammetric data for forest inventory purposes.

The objective of this study was to investigate the relationship between seasonality and different optical band configurations and prediction performance for common boreal tree species. Predicted variables were tree species proportions (0–1) and tree species volumes (m^3 ha^{-1}). Seasonality was considered by repeating data collection in spring, summer and autumn. A separate point cloud was created for each season from a consumer-grade camera and spectral data from a calibrated multispectral camera were attached to the point cloud data. The tested band configurations were red, green blue (RGB) and RGB complemented with red-edge and near infra bands (MS).

2 Material and methods

2.1 Study area

The 40-ha study area (62°36′ N; 29°2′ E) is located in the municipality of Liperi in eastern Finland (Fig. 1, Table 1). The forests in the study area are primarily used for timber production and are comprised of a mosaic of stands of different development stages and tree species composition. The development stages vary from recently felled and renewed forests to mature forests. The forests utilised for timber production are typically treated by thinning, at least twice during the rotation period, and the final felling is typically a clear-cut.

Table 1 Average growing stock volume, stem count, height of the basal area median tree (HGM), and diameter of the basal area median tree (DGM) in the field plots used in this study

	Pine	Spruce	Broadleaved	Total
Volume (m³/ha)	44.1	68.9	39.4	152.4
Stem count (n/ha)	201.8	580.1	384.9	1166.9
HGM (m)	17.9	13.6	15.0	16.0
DGM (cm)	21.2	16.7	14.9	18.8

Coniferous tree species are dominant in the study area (Fig. 2). The most common coniferous tree species are Scots pine (*Pinus sylvestris* [L.]) and Norway spruce (*Picea abies* [L.] Karst.). Broadleaved species, mostly birch (*Betula pendula* Roth. and *Betula pubescens* Ehrh.), are common as mixtures, although they can occur as a dominant species in fertile soil types. Other broadleaved species, such as aspen and alder (*Alnus* spp.) can also be found as mixtures.

2.2 Field data

Field data were collected during autumn 2020. Trees were measured from 160 circular plots having a radius of either 7.98 m (200 m^2) or 5.64 m (100 m^2). Plots were systematically sampled at approximately 50 m distance

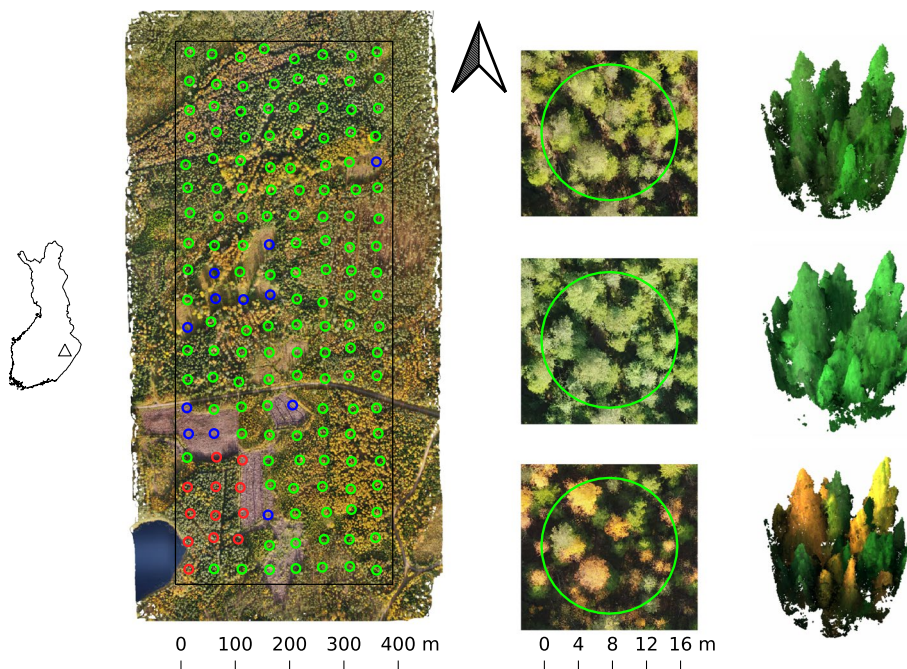**Fig. 1** Study area and locations of field plots(left). The complete orthophoto of the study area during autumn is shown. An example sample plot (centre) and point clouds (right) are also presented. Red circles (left) indicate plots that were excluded from the analysis due to forest management operations between data collections. Blue circles (left) indicate plots that were in seedling stands
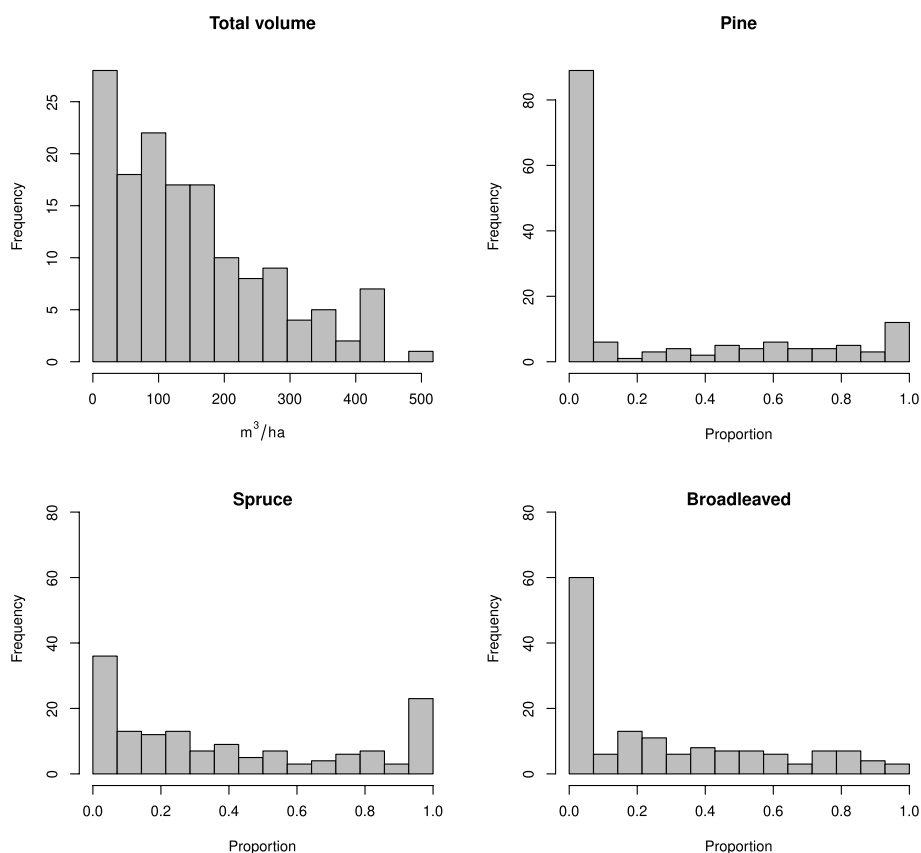
Kukkonen *et al. Annals of Forest Science*   (2024) 81:31

Page 4 of 13

Total volume

Pine

Spruce

Broadleaved

Fig. 2 Histograms of total volume and tree species proportions from the field plots used in this study

between plots (Fig. 1). The field team navigated to the plots with a consumer-grade GPS device and the final locations of the plot centres were randomised nearby the estimated location of the plot. The origin of the systematic plot network was randomised by placing the first plot (i.e., the upper left plot) at a random location. Plot centres were located using Trimble GeoXH with the Tornado antenna elevated to 5 m. Trees with a diameter at breast height (DBH) ≥ 10 cm were measured on the 200 m^2 plot, whereas trees with a DBH ≥ 5 cm but < 10 cm were measured on the 100 m^2 plot. For all trees, DBH was calipered, tree height was measured, and tree species determined. Individual tree volumes were estimated as a function of DBH and tree height using the species-specific models of Laasasenaho (1982). The tree volumes were summed within a plot and converted to the per hectare level (m^3 ha^{-1}), separately for both plot sizes. Then final plot-level volumes were obtained by summing volumes of two plot sizes. Plot-level volumes were calculated by tree species and for the total. Tree species in this study were Scots pine, Norway spruce and broadleaved trees. Tree species proportions (0–1) at the plot-level were calculated as a fraction of total volume. For instance, if the proportion

of Scots pine is 60% and the proportion of spruce is 40% in terms of volume, the species proportions are Scots pine $= 0.6$, Norway spruce $= 0.4$ and broadleaf $= 0.0$. As thinning was conducted at one of the forest stands during data collection (Fig. 1), 12 field plots had to be excluded from the analysis.

2.3 Image acquisition

The study area was photographed on three separate occasions from a DJI M210 quadcopter using a DJI X5S camera (hereafter X5S) and a MicaSense Altum MS camera (Tables 2 and 3). The two sensors were mounted on the drone at the same time, allowing for concurrent data collection. X5S was only used to create the photogrammetric point clouds for each season, whereas spectral information for all the analysis was derived from the Altum MS camera. The data acquisition dates were September 27th 2020 (autumn), May 17th 2021 (spring) and July 17th 2021 (summer). It was intended that the data be acquired in spring during leaf-off conditions, in the middle of the growing season, and during leaf senescence in autumn. This was successful in autumn and summer but data collection in spring was delayed due to late snow

Kukkonen *et al. Annals of Forest Science*   (2024) 81:31

Page 5 of 13

Table 2 Centre wavelengths and bandwidths of the Altum sensor. RGB denotes red–green–blue band configuration and MS denotes multispectral band configuration

Band	Centre (nm)	Bandwidth (nm)	Band configuration
Blue	475	32	RGB and MS
Green	560	27	RGB and MS
Red	668	14	RGB and MS
Red-edge	717	12	MS
Near-infrared	842	57	MS

Table 3 Specifications of the cameras used in this study. Values in parentheses represent the 35-mm equivalent focal length (mm) of the camera

Camera	Focal length (mm)	Sensor size (px)	Pixel size (μm)	Nominal GSD (cm)
Altum MS	8 (38.9)	2064×1544	3.45	4.3
DJI X5S	15 (30.0)	5280×3956	3.40	2.3

melt. Therefore, to avoid contamination of the reflectance by snowy patches, the spring data were instead collected at the period when the birch trees had begun to produce new leaves.

The sensor band configurations in this study were denoted as MS and RGB (Table 2), where RGB is a subset of bands from the Altum MS camera. The data acquisition parameters and flight plans were identical, and the same 10 ground control points (GCP) were used on all three occasions. These ground control points were located using the same procedure as in the case of field plots. As the data was collected simultaneously with the two cameras as the payload, the overlaps of the flight lines and consecutive images could only be planned for one of the cameras. Therefore, the flight parameters were selected based on the characteristics of the MS camera so that the lateral overlap of the MS images was 80% and the forward overlap was 80%. This resulted in a lateral overlap of 85% and a forward overlap of 85% for the DJI camera. Flying altitude was 100 m, which gave a nominal ground sampling distance (GSD) of 4.3 cm for the Altum camera and 2.3 cm for the X5S.

The entire study area was captured on a single day ± 2 h from the solar noon on all three occasions. The weather conditions were ideal, with little or no wind and a cloudless sky. The MS images of a reflectance panel were taken before and after each individual flight. These panel images were used to convert the pixel values of each MS image to reflectance values using the procedure recommended by MicaSense (MicaSense 2020), which were

clamped between 0 and 1 and quantised to unsigned short (0–65535). Thus, both RGB and MS band configurations contained reflectance data.

Altum records each band separately in individual files. After the conversion to reflectance, all bands of a single capture were co-aligned and merged into a single file. These become the MS images that were used in photogrammetric processing in Agisoft Metashape. The X5S images were not further processed prior to photogrammetric processing.

2.4 Photogrammetric point clouds
Photogrammetric point clouds were created from the X5S images using Agisoft Metashape (version 1.8.0, build 13,794) with "high" quality image alignment and "high" quality dense point cloud generation with "moderate" filtering. No photogrammetric point clouds were created from the MS images, but the exterior orientations of the MS images and internal orientation of the MicaSense Altum camera were exported from Metashape after the photos were aligned using the same Metashape parameter values as in the photogrammetric processing of X5S images. The same 10 ground control points were used in the processing of both X5S and MS images. Internal and external orientations were utilised in the fusion of the MS image data with the photogrammetric point cloud from the X5S camera using collinearity equations (see e.g. Packalen et al. 2009). For each point in the photogrammetric point cloud, collinearity equations were used to determine the images that contained each point. The average band value of all these images was attached to that point.

Finally, the photogrammetric point clouds from the three seasons were converted to above ground level using publicly available LiDAR data from the National Land Survey of Finland (NLS) (Maanmittauslaitos 2022). LiDAR data were ground filtered using the method described in Axelsson (2000), after which a triangulated irregular network (TIN) was formed from all the LiDAR points classified as ground. The interpolated value of the TIN was subtracted from every point in the photogrammetric point clouds.

2.5 Feature extraction
Various structural and optical features were computed from the ground normalised point cloud data. Features were computed for the field measured plots using a 7.98-m radius around the plot centre. Optical metrics included minimum, maximum, mean, median, standard deviation, skewness and kurtosis of each band. Structural metrics included minimum, maximum, mean, median, standard deviation, skewness, kurtosis, densities (1.3 m, 2.5 m, 5 m, 7.5 m, 10 m, 15 m, 20 m and 25 m)

and percentiles (10th, 20th, … 80th, 90th) of the height values of points within the plot boundaries. Only points located ≥ 2 m above the ground surface were considered in the computation of structural and optical metrics. Field plots with fewer than 10 points ≥ 2 m above ground surface were excluded. This resulted in a total of 136 field plots for the analysis.

2.6 Modelling

This study utilised two different categories of predictor variables calculated from the point cloud data: structural and optical. Of these, only optical features, i.e. features calculated from the reflectance values of the different bands of the Altum sensor (Table 2), were used in the zero–one inflated beta (ZOIB) regression models of tree species proportions. Such an approach facilitated the assessment of the influence that the different optical bands had on the prediction of tree species using a permute-and-relearn approach. Tree species volumes were predicted with Gaussian process regression (GPR), which utilised both structural and optical features.

2.6.1 Zero–one inflated beta regression

The proportions of pine, spruce and broadleaved tree species were predicted separately. Each species was predicted using ZOIB regression as implemented in the R (R Core Team 2022) package gamlss (Rigby and Stasinopoulos 2005). The inflated beta distribution is similar to the beta distribution Beta(α,β) on (0,1), but it also allows, in addition for zeros and ones of the response variable (species proportion) through modelling, the probability of zero, p_0, and the probability of one, p_1. Standardised average values of 1) the RGB bands, or 2) the MS bands were used as the predictor variables through a linear model for $v = p_0/p_2$ and $\tau = p_1/p_2$ with $p_2 = 1 - p_0 - p_1$, and through a logistic model for $\mu = \alpha/(\alpha+\beta)$. The parameter $\sigma = 1/(\alpha+\beta+1)$ was assumed constant. Here, $0 < \mu < 1$, $0 < \sigma < 1$, $v > 0$ and $\tau > 0$. As a result, each plot was attached with a ZOIB distribution. We summarised this distribution to a single predicted value as follows:

$$\begin{cases} 0 & \text{if } \widehat{p}_0 = \widehat{v}/\left(1 + \widehat{v} + \widehat{\tau}\right) > 0.5 \\ 1 & \text{if } \widehat{p}_1 = \widehat{\tau}/\left(1 + \widehat{v} + \widehat{\tau}\right) > 0.5 \\ \widehat{\mu} & \text{otherwise,} \end{cases}$$

where $\widehat{v}$, $\widehat{\tau}$ and $\widehat{\mu}$ are estimated parameter values. Finally, the predicted tree species proportions were scaled at each plot to sum to 1 (each proportion was divided by the sum of proportions). Root mean square error (RMSE) was used as a metric for the prediction errors for the proportions of tree species.

2.6.2 Band importance

Band importance was computed using ZOIB regression with a permute-and-relearn approach (Hooker et al. 2021) with tree species proportion assigned as the dependent variable and the average values of the bands at the plot-level assigned as predictor variables. One input feature (i.e., average value of a band at the plot-level) was permuted at a time, the ZOIB regression model was refit, and the resulting prediction error recorded. This process was repeated 100 times for each input feature and the importance of a feature with respect to tree species proportion was the average difference in prediction error compared to the scenario where no input features were permutated. Band importance was investigated for RGB and MS data separately.

2.6.3 Multivariate Gaussian process regression

Tree species volumes were predicted using GPR, which is a kernel-based regression method that models the data using multivariate Gaussian distribution (Rasmussen and Williams 2006). The multivariate version of GPR (MGPR) enables the simultaneous prediction of several attributes, which is a common requirement in forest inventories. Here, the volumes of all tree species were predicted simultaneously. The predictive performance of MGPR has shown promise in forest attribute predictions by tree species (Varvia et al. 2019).

The key element of GPR is a covariance function/kernel that defines the flexibility of the fitted model and how strictly the model pursues to learn training data. We used a stationary Matérn 2/3 covariance function in this study. The kernel hyperparameters (kernel variance, error variance, and length scale parameter) were optimised using a heuristic approach that uses k-fold cross-validation. The average of the species-specific root mean square error (RMSE) values was used as a cost in the optimisation of hyperparameters, and the zero-mean function was used as a mean function of a model. Negative predictions were corrected following the procedure proposed in Varvia et al. (2019).

The R package *mgpr* (Varvia et al. 2023) was utilised in this study as the implementation of MGPR. The prediction of tree species volumes was carried out using structural and optical features. Variable selection was not necessary with MGPR, but we reduced the dimensions of the feature space by excluding highly collinear features (|cor| > 0.95) prior to fitting the MGPR models. The models were validated using 10-fold cross-validation that was iterated 100 times. Repeated cross-validations were used to avoid the results being dependent on the random splits. Relative RMSE (%RMSE) was used as a metric for the prediction errors for volumes by tree species.

Kukkonen *et al. Annals of Forest Science*   (2024) 81:31

Page 7 of 13

3 Results

Band importance for the MS and RGB data is presented in Figs. 3 and 4, respectively. In summer, the green and red-edge bands appeared to be of considerable importance for the prediction of the proportion of broadleaves. However, when only the RGB bands were considered, none of the bands appeared to have a substantial impact. In autumn, the blue band appeared to be relatively important when predicting the proportion of pine trees with both MS and RGB data.

Scatterplots of the tree species proportions predicted with ZOIB regression are presented in Fig. 5. Corresponding RMSE values can be found in Table 4. The differences between the RGB and MS data in the different seasons and for all tree species were notable. The benefit of using MS data was most apparent when predicting the proportion of broadleaved tree species in summer and spring, and when predicting the proportion of spruce

trees in summer. In autumn, however, the differences between the RGB and MS data were minor. In summer, the RGB data resulted in a prediction error for broadleaves that was over twice as high as produced by the MS data, whereas in autumn the difference between the band configurations was very small. Of all the considered tree species, pine was the least affected by band configuration or seasonality, while broadleaves were most affected by both band configuration and seasonality.

The scatterplots of tree species volumes predicted with MGPR are presented in Fig. 6. Corresponding %RMSE values can be found in Table 5. These results are, for the most part, in line with the ZOIB regression prediction errors associated with species proportions. Here, pine was also the least affected by band configuration, while broadleaves were the most affected. Sensor band configuration had no noticeable influence on the prediction error associated with total tree volume.
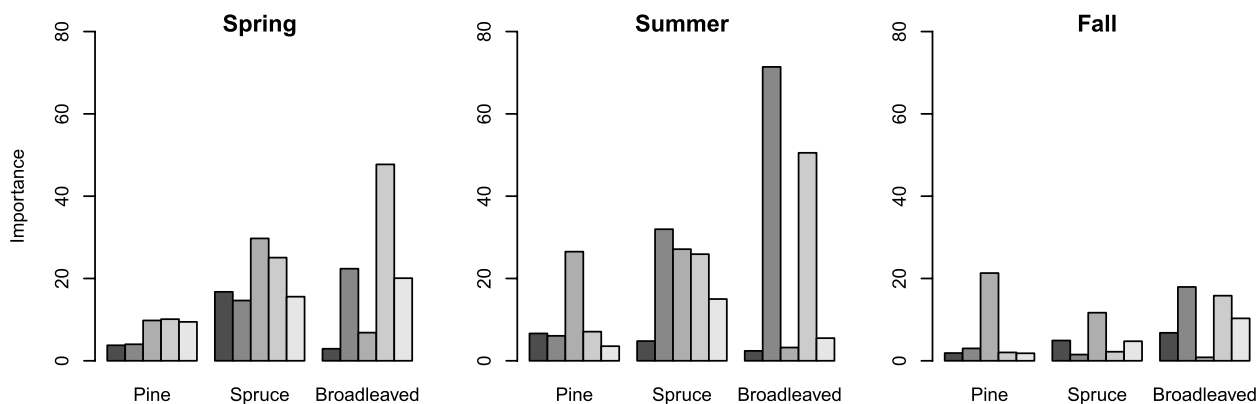

Fig. 3 Multispectral **(**MS) band importance computed with the permute-and-relearn approach. Bars from left to right are red, green, blue, red-edge and near-infrared. *Y*-axis represents the importance calculated as the average absolute difference in root mean square error (RMSE) of tree species proportion over 100 band permutation iterations
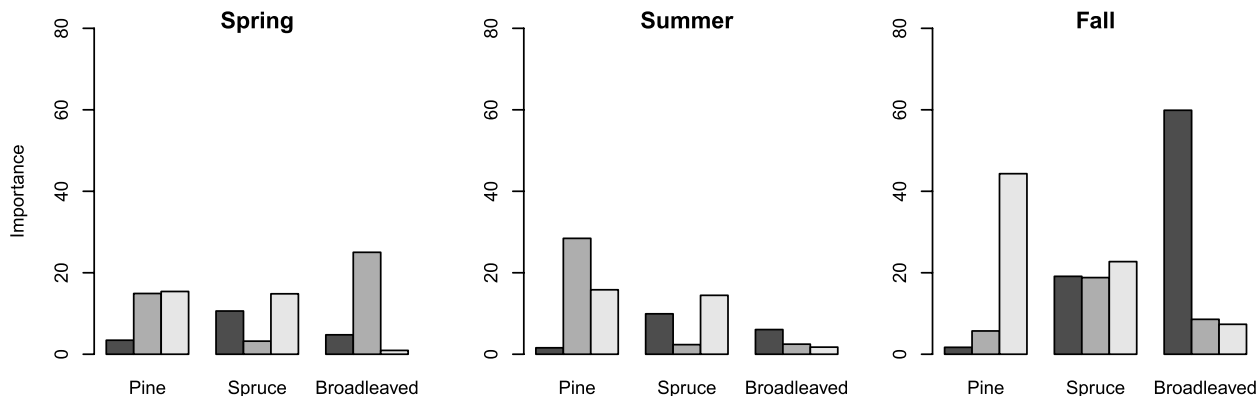

Fig. 4 Red-blue-green (RGB) band importance computed with the permute-and-relearn approach. Bars from left to right are red, green, and blue. *Y*-axis represents the importance calculated as the average absolute difference in root mean square error (%RMSE) of tree species proportion over 100 band permutation iterations
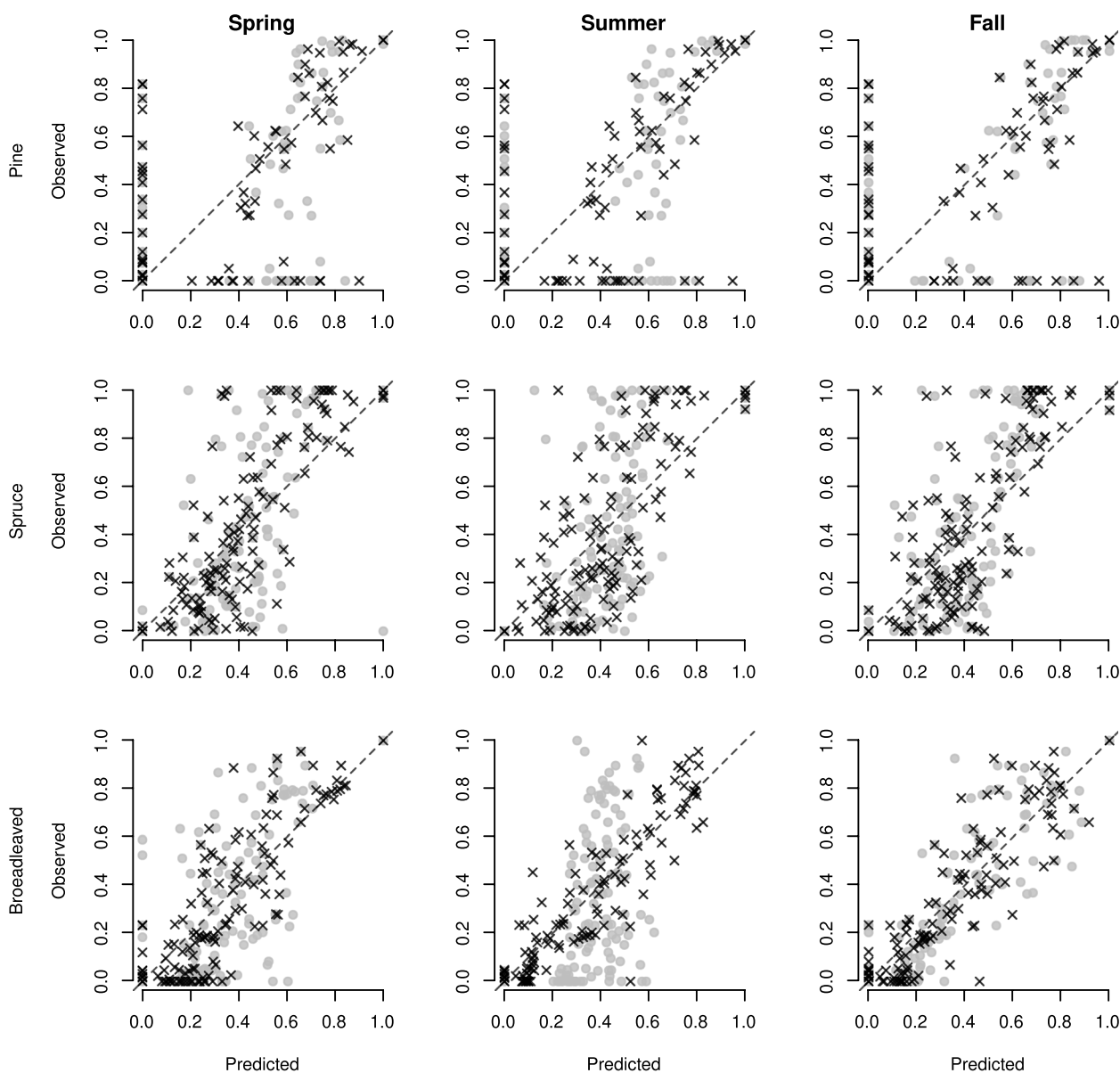
Fig. 5 Scatterplots of zero–one inflated beta (ZOIB) regression predictions of tree species proportions and field-measured tree species proportions. Grey dots represent ZOIB regression models when only red-blue-green (RGB) data were used, and black crosses represent ZOIB regression models when multispectral (MS) data were used. No structural predictor variables were used. Dashed line is the 1:1 line

However, total tree volume was predicted with less error using the autumn data than with data from the other two seasons.

There were also some noticeable differences in the species proportion results. Spruce volume was predicted with substantially less error in autumn than in the other seasons. In contrast, pine volume was predicted with a noticeably greater error in spring than in the other seasons. Also, while the proportion of

broadleaves in spring was predicted with much less error with the MS data, the corresponding difference in the prediction error associated with tree volume was small.

It is reasonable to assume that these differences are due to the change in the structure of the point cloud caused by phenology or other seasonal factors, because a similar phenomenon was not present when tree species proportions were predicted using only optical features (Fig. 5 and Table 4).

Kukkonen *et al. Annals of Forest Science*   (2024) 81:31

Page 9 of 13

Table 4 Root mean square error (RMSE) values of zero–one inflated beta (ZOIB) regression predictions of tree species proportions. The Pearson correlation coefficient between predicted and observed values is presented in parenthesis after the RMSE values. RGB indicates that red–green–blue data were used, and MS indicates that multispectral data were used in addition to red–green–blue data. Values in bold indicate the lowest prediction error for that sensor configuration and tree species

	Bands	Spring	Summer	Autumn
Pine	RGB	0.27 (0.67)	**0.26 (0.69)**	**0.26 (0.69)**
	MS	0.25 (0.73)	**0.24 (0.75)**	**0.24 (0.75)**
Spruce	RGB	0.26 (0.67)	0.28 (0.59)	**0.25 (0.69)**
	MS	**0.21 (0.80)**	0.22 (0.77)	0.24 (0.74)
Broadleaved	RGB	0.25 (0.57)	0.27 (0.46)	**0.17 (0.83)**
	MS	0.16 (0.84)	**0.13 (0.90)**	0.15 (0.87)

4 Discussion

4.1 Data acquisition

All flights were conducted continuously in a single day and included the capture of a calibration image of a reflectance panel before take-off and after landing. All data acquisitions were conducted within 2 h of the local solar noon on windless days with a clear sky, thus eliminating the influence that variable weather conditions might have on the results.

Spring data were planned to be collected during a completely leaf-off period. However, due to late snow melt in the study area, the data were instead collected at a time when the broadleaves (mainly birch) were beginning to produce new leaves (see Fig. 1). This is a typical situation when collecting leaf-off data in many boreal regions, i.e. the timing of snow melt determines when optical data acquisition is possible in spring. Similarly, the time frame for optimal data acquisitions during autumn is affected by, among other factors, weather conditions that vary from 1 year to another. In this study, data acquisition during autumn was determined by visiting the study area several times and commencing data acquisition only when the stage of leaf colourization (based on visual inspection) was similar for most of the deciduous trees. However, it should be noted that the timings of data acquisitions in this study were planned for specific periods during growing season and cannot repeated as such in operational inventories, where the efficiency of the data acquisition is of major importance.

4.2 Tree species proportions

Tree species proportions were predicted with comparable accuracy in previous studies. Using MS data

during summer, the RMSE values ranged from 0.13 to 0.24 depending on the tree species. For example, Puliti et al. (2017) used photogrammetric point cloud data from aerial images and report RMSE values ranging from 0.12 to 0.21 depending on the tree species and image overlap. Independent of the season or the considered tree species, tree species proportions were predicted with less error when using MS data compared to RGB data. The magnitude of the difference in prediction error varied with tree species and data acquisition dates. The MS data were much less affected by the seasonality of the data than the RGB data. Overall, the MS data had marginally lower prediction errors with summer data acquisition compared to other seasons, whereas this period was found to be much less suitable for RGB data. This suggests that the intraspecific variation in MS reflectance was minimal in the middle of the growing season and that MS data captured the interspecific variation in reflectance better than RGB data during this period. Such a conclusion is supported by the results of band importance (Figs. 3 and 4), where red-edge band is highly important during the summer for the discrimination of broadleaved trees. Furthermore, the importance of the near-infrared range of the electromagnetic spectrum for the discrimination of tree species has been highlighted by earlier studies (see e.g. Packalén et al. 2006, Immitzer et al. 2012). Moving to autumn, these bands became less important, perhaps due to the advancing leaf colourization that alters the spectral properties both within tree species (Blackburn and Milton 1995) and across different tree species (Key et al. 2001).

The RGB data produced slightly greater prediction errors in autumn compared to the MS data in summer. Thus, the leaf senescence period provided a time window in which the considered tree species were predicted more accurately than at other times, using only the visible wavelength spectrum. The operational implication from the perspective of forest inventories is that lower cost data acquisition equipment could be used during autumn. In fact, UAS can be particularly useful in such situations since the area coverage is generally quite limited and phenology can have large variation in larger areas where ecological gradients exist (Cole and Sheldon 2017). Regardless, the intraspecific variation in phenology during autumn influences the prediction of tree species proportions when MS data is used.

4.3 Tree species-specific volumes

Interpretation of the errors associated with the prediction of tree species is different to the interpretation of the errors associated with tree species proportions in the sense that the seasonal differences of the photogrammetric point clouds also influence the results. The prediction
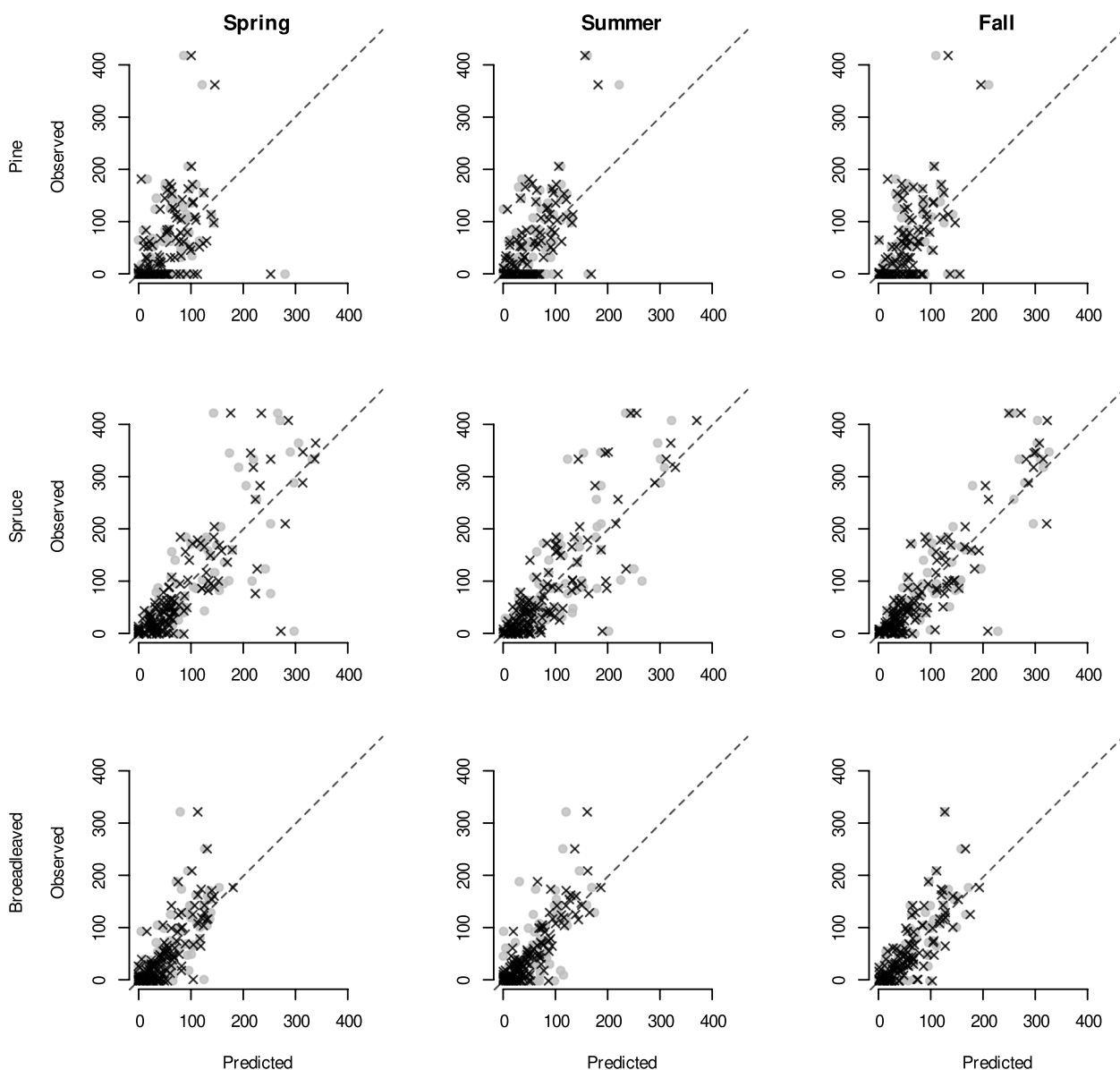
Fig. 6 Scatterplots of multivariate Gaussian process regression (MGPR) predictions of species-specific tree volumes (m^3/ha). Grey dots are produced by the MGPR models where, in addition to structural features, red–green–blue (RGB) data were used. Black crosses are produced from the MGPR models where multispectral (MS) data were used in addition to structural features. The predictions are the average predicted value of 10-fold cross-validation iterated 100 times. Dashed line is the 1:1 line

errors of volumes by tree species (ranging from 30.85 to 61.80%) are comparable to other studies where volumes by tree species were predicted using photogrammetric UAS data (Kukkonen et al. 2021; Tuominen et al. 2017). Kukkonen et al. (2021) report %RMSE values ranging between 33.4 and 62.6% for the same tree species classes as were used in this study. Similarly, Tuominen et al. (2017) obtained %RMSE values between 34.5 and 57.2%.

Bohlin et al. (2017) have noted that the use of leaf-off photogrammetric point cloud data can lead to a

noticeable underestimation of tree volume in deciduous-dominated areas. In our study, the prediction error associated with the volume of broadleaves was greatest in spring, although the difference between RGB and MS was relatively minor (41.31% vs. 38.73%, respectively), in contrast to the prediction of broadleaf proportions in spring (0.24 vs. 0.16). This would suggest that either phenology or other environmental factors, such as sun angle and shadows, influence the structure of the point cloud in a manner that complements the absence of a near-infrared

Table 5 Root mean square error (%RMSE) values of multivariate Gaussian process regression (MGPR) predictions of species-specific tree volumes. The Pearson correlation coefficient between predicted and observed values is presented in parenthesis after the RMSE values. RGB indicates that red–green–blue data were used, and MS indicates that multispectral data were used, in addition to structural features. The %RMSE values are calculated using the average predicted value from 10-fold cross-validation iterated 100 times for each plot. Values in bold indicate the lowest prediction error for that sensor configuration and tree species

	Bands	Spring	Summer	Autumn
Pine	RGB	61.80 (0.48)	**50.82 (0.68)**	53.65 (0.62)
	MS	60.90 (0.53)	**49.88 (0.68)**	52.52 (0.63)
Spruce	RGB	59.85 (0.81)	57.34 (0.82)	**45.18 (0.89)**
	MS	56.41 (0.85)	52.33 (0.86)	**43.79 (0.90)**
Broadleaved	RGB	41.31 (0.73)	40.99 (0.72)	**33.51 (0.83)**
	MS	38.73 (0.80)	**30.85 (0.86)**	34.41 (0.82)
Total	RGB	26.58 (0.93)	25.05 (0.94)	**23.07 (0.95)**
	MS	26.60 (0.93)	25.01 (0.94)	**23.45 (0.95)**

spectrum of radiation for the prediction of broadleaved tree volumes. Regarding phenology, it is likely that the advancing, yet not finished leaf-flush improves the discrimination of broadleaves and conifer trees because of the changing characteristics of photogrammetric point cloud data. This conclusion is supported by previous research where the benefit of leaf-off point cloud data for the discrimination of broadleaved trees has been shown using both airborne lidar (Villikka et al. 2012) and photogrammetric (Bohlin et al. 2016) data.

The errors associated with the prediction of pine and spruce volumes were strongly affected by seasonality. However, these errors differ from the errors associated with broadleaved trees as the band configuration was found to have very little effect on the prediction errors. This would indicate that only the structural differences of the point clouds between seasons affect the errors associated with the prediction of pine and spruce volumes. It should be noted that the study area is slightly unconventional in a Finnish context, as it contains quite much broadleaved trees (Table 1, Fig. 1). This could have had an exaggerated effect on the point cloud structure in the spring data, which could have led to the increased prediction errors associated with pines.

However, there are a few differences, related to phenology, between summer and autumn that influence the structure of the point cloud and that could explain the lower prediction errors associated with spruce during this season. We hypothesise that the abundance of shadows, caused by the lower sun angle during autumn, affects the characteristics of the point cloud. It is worth noting here that all photogrammetric point clouds were normalised to the ground surface using auxiliary LiDAR data. Thus, the varying number of ground points in photogrammetric point clouds in different seasons does not affect the normalisation process in any way.

5 Conclusion

The influence of both seasonality (spring, summer or autumn) and sensor band configuration (conventional RGB, and RGB complemented with red-edge and near-infrared bands) for tree species prediction was investigated in this study. The MS data was found to be much less affected by seasonality than the RGB data. If the band configuration of the sensor is limited to conventional RGB, a period during which leaf colourization is at its later stages, could provide significantly better tree species discrimination than a similar data collection during summer. Furthermore, it was found that differences in the structure of the point cloud in between seasons may affect the prediction errors of volumes by tree species. The results provide insights and recommendations for the suitability of different sensors and seasons for tree species-specific forest inventories using an UAS platform over a relatively small (forest estate level) inventory area. Future research should focus on a wider range of forest types, tree species compositions and gradients in phenology.

Authors' contributions

Mikko Kukkonen: conceptualization, data curation, formal analysis, investigation, methodology, software, validation, writing—original draft, writing—review and editing. Mari Myllymäki: dormal analysis, Investigation, methodology, software, validation, writing—original draft, writing—review and editing. Janne Räty: investigation, software, writing—original draft, writing—review and editing. Petri Varvia: investigation, software, writing—original draft, writing—review and editing. Matti Maltamo: conceptualization, investigation, writing—original draft, writing—review and editing. Lauri Korhonen: conceptualization, investigation, writing—original draft, writing—review and editing. Petteri Packalen: conceptualization, formal analysis, funding acquisition, investigation, methodology, software, supervision, validation, writing—original draft, writing—review and editing. The authors read and approved the final manuscript.

Availability of data and materials

The datasets generated during and/or analysed during the current study are available from the corresponding author on reasonable request.

Code availability

The custom code and/or software application generated during and/or analysed during the current study are available from the corresponding author on reasonable request.

Kukkonen *et al. Annals of Forest Science*   (2024) 81:31

Page 12 of 13

Declarations

Author details
[1]Natural Resources Institute Finland (Luke), Bioeconomy and Environment Unit, Yliopistokatu 6, 80130 Joensuu, Finland. [2]Natural Resources Institute Finland (Luke), Bioeconomy and Environment Unit, Latokartanonkaari 9, 00790 Helsinki, Finland. [3]School of Forest Sciences, University of Eastern Finland, P.O. Box 111, 80101 Joensuu, Finland.

References

Axelsson PE (2000) DEM generation from laser scanner data using adaptive TIN models. Int Arch Photogrammetry Remote Sens 33:110–117

Blackburn GA, Milton EJ (1995) Seasonal variations in the spectral reflectance of deciduous tree canopies. Int J Remote Sens 16(4):709–720

Bohlin J, Wallerman J, Fransson JES (2016) Deciduous forest mapping using change detection of multi-temporal canopy height models from aerial images acquired at leaf-on and leaf-off conditions. Scand J for Res 31(5):517–525. https://doi.org/10.1080/02827581.2015.1130850

Bohlin J, Bohlin I, Jonzén J (2021) Nilsson M (2017) Mapping forest attributes using data from stereophotogrammetry of aerial images and field data from the national forest inventory. Silva Fenn 51(2):18. https://doi.org/10.14214/sf.2021

Brockerhoff EG, Barbaro L, Castagneyrol B et al (2017) Forest biodiversity, ecosystem functioning and the provision of ecosystem services. Biodivers Conserv 26:3005–3035. https://doi.org/10.1007/s10531-017-1453-2

Cho MA, Mathieu R, Asner GP, Naidoo L, Van Aardt J, Ramoelo A, Debba P, Wessels K, Main R, Smit IP (2012) Mapping tree species composition in South African savannas using an integrated airborne spectral and LiDAR system. Remote Sens Environ 125:214–226

Cole EF, Sheldon BC (2017) The shifting phenological landscape: Within- and between-species variation in leaf emergence in a mixed-deciduous woodland. Ecol Evol 7:1135–1147. https://doi.org/10.1002/ece3.2718

Grabska E, Socha J (2021) Evaluating the effect of stand properties and site conditions on the forest reflectance from Sentinel-2 time series. PLoS ONE 16(3):e0248459. https://doi.org/10.1371/journal.pone.0248459

Hardenbol A, Kuzmin A, Korhonen L, Korpelainen P, Kumpula T, Maltamo M, Kouki J (2021) Detection of aspen in conifer-dominated boreal forests with seasonal multispectral drone image point clouds. Silva Fennica 55:4. https://doi.org/10.14214/sf.10515

Hill RA, Wilson A, George M, Hinsley S (2010) Mapping tree species in temperate deciduous woodland using time-series multi-spectral data. Appl Veg Sci 13:86–99. https://doi.org/10.1111/j.1654-109X.2009.01053.x

Hooker G, Mentch L, Zhou S (2021) Unrestricted permutation forces extrapolation: variable importance requires at least one more model, or there is no free variable importance. Stat Comput 31:82. https://doi.org/10.1007/s11222-021-10057-z

Hovi A, Raitio P, Rautiainen M (2017) A spectral analysis of 25 boreal tree species. Silva Fenn 51(4):7753. https://doi.org/10.14214/sf.7753

Huang H, He S, Chen C (2019) Leaf abundance affects tree height estimation derived from UAV images. Forests 10(10):931. https://doi.org/10.3390/f10100931

Hynynen J, Ojansuu R, Hökkä H, Siipilehto J, Salminen H, Haapala P (2002) Models for predicting stand development in MELA System. Finn for Res Inst Res Pap 835:1–116

Immitzer M, Atzberger C, Koukal T (2012) Tree species classification with random forest using very high spatial resolution 8-band WorldView-2 satellite data. Remote Sens 4(9):2661–2693. https://doi.org/10.3390/rs4092661

Key T, Warner TA, McGraw JB, Fajvan MA (2001) A comparison of multispectral and multitemporal information in high spatial resolution imagery for classification of individual tree species in a temperate hardwood forest. Remote Sens Environ 75(1):100–112

Kobayashi H, Nagai S, Kim Y, Yang W, Ikeda K, Ikawa H, Nagano H, Suzuki R (2018) In situ observations reveal how spectral reflectance responds to growing season phenology of an open evergreen forest in Alaska. Remote Sens 10(7):1071. https://doi.org/10.3390/rs10071071

Kukkonen M, Kotivuori E, Maltamo M, Korhonen L, Packalen P (2021) Volumes by tree species can be predicted using photogrammetric UAS data, Sentinel-2 images and prior field measurements. Silva Fenn 55(1):10360. https://doi.org/10.14214/sf.10360

Laasasenaho J (1982) Taper curve and volume functions for pine, spruce and birch. Communicationes Instituti Forestalis Fenniae 108:1–74

Lisein J, Michez A, Claessens H, Lejeune P (2015) Discrimination of deciduous tree species from time series of unmanned aerial system imagery. PLoS One 10(11):e0141006. https://doi.org/10.1371/journal.pone.0141006

Maanmittauslaitos (2022) Laserkeilausaineisto 5p. Available at https://www.maanmittauslaitos.fi/kartat-ja-paikkatieto/asiantuntevalle-kayttajalle/tuotekuvaukset/laser-scanning-data-5-p. Accessed 11 Nov 2022

Masaitis G, Mozgeris G, Augustaitis A (2013) Spectral reflectance properties of healthy and stressed coniferous trees. iForest. 6:30–36. https://doi.org/10.3832/ifor0709-006

MicaSense (2020) https://support.micasense.com/hc/en-us/articles/115000351194-Radiometric-Calibration-Model-for-MicaSense-Sensors. Accessed 20 Feb 2020

Noda HM, Muraoka H, Nasahara KN (2021) Plant ecophysiological processes in spectral profiles: perspective from a deciduous broadleaf forest. J Plant Res 134:737–751. https://doi.org/10.1007/s10265-021-01302-7

Packalen P, Suvanto A, Maltamo M (2009) A two stage method to estimate species-specific growing stock. Photogramm Eng Remote Sens 75:1451–1460. https://doi.org/10.14358/PERS.75.12.1451

Packalén P, Maltamo M (2006) Predicting the plot volume by tree species using airborne laser scanning and aerial photographs. Forest Sci 52(6):611–622. https://doi.org/10.1093/forestscience/52.6.611

Persson M, Lindberg E, Reese H (2018) tree species classification with multi-temporal sentinel-2 data. Remote Sens 10(11):1794. https://doi.org/10.3390/rs10111794

Pu R (2021) Mapping tree species using advanced remote sensing technologies: a state-of-the-art review and perspective. J Remote Sens 2021:9812624. https://doi.org/10.34133/2021/9812624

Puliti S, Gobakken T, Ørka HO, Næsset E (2017) Assessing 3D point clouds from aerial photographs for species-specific forest inventories. Scand J for Res 32(1):68–79. https://doi.org/10.1080/02827581.2016.1186727

R Core Team (2022) R: A language and environment for statistical computing. R Foundation for Statistical Computing, Vienna, Austria. https://www.R-project.org/

Rasmussen C, Williams K (2006) Gaussian Processes for Machine Learning. The MIT Press

Rigby RA, Stasinopoulos DM (2005) Generalized additive models for location, scale and shape. J Roy Stat Soc Ser C (Appl Stat) 54:507–554. https://doi.org/10.1111/j.1467-9876.2005.00510.x

Salas-Eljatib C, Mehtätalo L, Gregoire TG, Soto DP, Vargas-Gaete R (2021) Growth equations in forest research: mathematical basis and model similarities. Curr Forest Rep 7:230–244

Siefert A, Violle C, Chalmandrier L et al (2015) A global meta-analysis of the relative extent of intraspecific trait variation in plant communities. Ecol Lett 18:1406–1419. https://doi.org/10.1111/ele.12508

Tuominen S, Balazs A, Honkavaara E, Pölönen I, Saari H, Hakala T, Viljanen N (2017) Hyperspectral UAV-imagery and photogrammetric canopy height model in estimating forest stand variables. Silva Fennica 51(5):7721. https://doi.org/10.14214/sf.7721

Varvia P, Lähivaara T, Maltamo M, Packalen P, Seppänen A (2019) Gaussian process regression for forest attribute estimation from airborne laser

scanning data. IEEE Trans Geosci Remote Sens 57(6):3361–3369. https://doi.org/10.1109/TGRS.2018.2883495

Varvia P, Räty J, Packalen P (2023) mgpr: An R package for multivariate Gaussian process regression. SoftwareX 24:101563. https://doi.org/10.1016/j.softx.2023.101563

Villikka M, Packalén P, Maltamo M (2012) The suitability of leaf-off airborne laser scanning data in an area-based forest inventory of coniferous and deciduous trees. Silva Fenn. 46:99–110

Weil G, Lensky IM, Resheff YS, Levin N (2017) Optimizing the timing of unmanned aerial vehicle image acquisition for applied mapping of woody vegetation species using feature selection. Remote Sens 9(11):1130. https://doi.org/10.3390/rs9111130

Wolter PT, Mladenoff DJ, Host GE, Crow TR (1995) Improved forest classification in the Northern Lake States using multi-temporal Landsat imagery. Photogramm Eng Remote Sens 61(9):1129–1143

Publisher's Note

Springer Nature remains neutral with regard to jurisdictional claims in published maps and institutional affiliations.